Manuscript prepared for Clim. Past
with version 5.0 of the LATEX class copernicus.cls.
Date: 22 December 2014

Variability of summer humidity during the past 800 years on the eastern Tibetan Plateau inferred from δ^{18}O of tree-ring cellulose

Jakob Wernicke[1], Jussi Grießinger[1], Philipp Hochreuther[1], and Achim Bräuning[1]

[1]Institute of Geography, Friedrich-Alexander-University Erlangen-Nuremberg

Correspondence to: Jakob Wernicke (jakob.wernicke@fau.de)

Abstract.
We present an 800 years long δ^{18}O chronology from the eastern part of the Tibetan Plateau (TP). The chronology dates back to 1193 AD and was sampled in 1996 AD from living *Juniperus tibetica* trees. This first long-term tree-ring based δ^{18}O chronology for eastern Tibet provides a reliable archive for hydroclimatic reconstructions. Highly significant correlations were obtained with hydroclimatic variables (relative humidity, vapour pressure and precipitation) during the summer season. We applied a linear transfer model to reconstruct summer season relative humidity variations over the past 800 years. More moist conditions prevailed during the termination of the Medieval Warm Period while, a systematic shift during the Little Ice Age is not detectable. A distinct trend towards more dry conditions is apparent since the 1870s. The moisture decline wakens around the 1950s but still shows a weak negative trend. The mid-19th century humidity decrease is in good accordance with several multiproxy hydroclimate reconstructions for south Tibet. However, the pronounced summer relative humidity decline is stronger on the central and eastern TP. Furthermore, the relative humidity at our study site is significantly linked to the relative humidity at large parts of the TP. Therewith we deduce that the reconstructed relative humidity is mostly controlled by local and mesoscale climatic drivers, although significant connections to the higher troposphere of west-central Asia were observed.

1 Introduction

The variation in strength, timing and duration of the Asian summer monsoon (ASM) system affects life and economy of many millions of people living in south and east Asia (Immerzeel et al. (2010); Zhang et al. (2008)). In remote areas, such as the Tibetan Plateau (TP), reliable climate records are short and scattered. Nevertheless, a recent weakening trend of the ASM precipitation amount was reported in several studies (Bollasina et al. (2011); Sano et al. (2011); Zhou et al. (2008b)). The decline in air humidity was explained by a reduction in the thermal gradient between the surface temperatures of the Indian Ocean and the TP due to Global Warming (Sun et al., 2010). Contemporaneously, different locations and climate archives reveal a strengthened monsoonal precipitation (Anderson et al. (2002); Kumar et al. (1999); Zhang et al. (2008)). This discrepancy may be explained by the high variability of the monsoon circulation itself, but also due to a limited number of available palaeoclimate studies and resulting climate modeling uncertainties. Thus, for a better understanding of the circulation system as a whole, but also for the verification of climate change scenarios, a keen demand for reliable climate reconstructions exists for the TP. With increasing numbers of palaeoclimatic records, forecast and climate projection precision increases and can be helpful to facilitate targeted decision making regarding water and resource management.

The northward movement of the Intertropical Convergence Zone (ITCZ) on the Northern Hemisphere in boreal summer is amplified over the Asian continent by the thermal contrast between the Indian Ocean and the TP (Webster et al., 1998). Convective rainfalls during the summer monsoon season between June and September are strongly altered by the complex topography of the Himalayas and western Chinese mountain systems (e.g. Böhner (2006); Maussion et al. (2014); Thomas and Herzfeld (2004)). Extreme climatic events that may have devastating effects, but also long-term trends of ASM intensity are therefore in the focus of numerous climate reconstruction efforts (e.g. Cook et al. (2010); Xu et al. (2006b); Yang et al. (2003)). Most of these studies use tree-ring width as a proxy for palaeoclimate reconstructions. Nonetheless, several studies demonstrated that δ^{18}O of wood cellulose is a strong indicator of hydroclimatic conditions (McCarroll and Loader (2004); Roden et al. (2000); Saurer et al. (1997) ; Sternberg (2009)). Even if tree stands might have been influenced by external disturbances (e.g. competition, insect attacks or geomorphological processes) they still reflect variations of the local hydroclimate accurately (Sano et al., 2013). Recently published tree-ring δ^{18}O chronologies from the TP show a common strong response to regional moisture changes. Grießinger et al. (2011) successfully reconstructed August precipitation over the past 800 years. They demonstrated reduced precipitation during the Medieval Warm Period (MWP), stronger rainfalls during the Little Ice Age (LIA), decreasing precipitation rates since the 1810s , and slightly wetter conditions after 1990s. In addition, shorter δ^{18}O chronologies from the central Himalayas showed consistent negative correlations to summer precipitation (Sano et al. (2010); Sano et al. (2011); Sano et al. (2013)). The detected recent reduction of monsoonal precipitation has been interpreted as a reaction to increased sea surface temperatures over the tropical Pacific and Indian Ocean (Zhou et al., 2008a). Strong responses to regional cloud cover changes were found for tree-ring δ^{18}O chronologies from the south-eastern TP (Liu et al. (2013); Liu et al. (2014); Shi et al. (2012)). The local moisture reduction since the middle of the 19th century is less pronounced than for south-west Tibet and was associated with complex El Niño-Southern oscillation teleconnections (Liu et al., 2012). Existing tree-ring δ^{18}O chronologies on the north-eastern part of the TP respond to local precipitation and relative humidity (Wang et al. (2013); Liu et al. (2008)). Except for a relatively short summer moisture sensitive time series (An et al., 2014), no long-term δ^{18}O chronologies and reliable reconstruction have been conducted for the eastern TP so far. It still remains unclear to what extent the MWP, LIA, and the modern humidity decrease are reflected in tree-ring δ^{18}O on the eastern TP, where the influence of the ASM, the Indian Summer monsoon and the westerlies overlap.

We present a new, well replicated 800 years long δ^{18}O chronology, representing a unique archive for studying the past hydroclimate in eastern Tibet. We applied response and transfer functions and obtained a reliable reconstruction of summer relative humidity (July+August). We compared the long-term trend of our chronology to other moisture sensitive proxy archives from several sites over the TP and discuss climatic control mechanisms on the relative humidity.

2 Material and methods

2.1 Study site - Lhamcoka

Lhamcoka is located on the eastern TP (see Figure 1 green pentagon). During a field campaign in 1996, 16 living *Juniperus tibetica* trees were cored twice in order to enhance the chance of detecting missing rings. The samples were collected from a steep, south-east exposed slope at an elevation of 4350m asl (31°49'N/99°06'E). The oldest tree is 801 years old, resulting in an overall chronology time span of 1193-1996 AD. The average single core length is 633 years with single segment lengths of 801a, 697a, 668a, 528a, and 469a, respectively. The chronology is not biased by an age trend as it was supposed for different high altitude mountain ecosystems (Esper et al. (2010); Treydte et al. (2006). We applied a spline based trend analysis and revealed non systematic trends during the first 100 years after germination (graph not shown here). Therefore a "juvenile" effect is not likely to affect our chronology, justifying the retention of the oldest parts of each single core. Juniper forms the upper timberline in the region due to its cold temperature tolerance (Bräuning, 2001). The species' annual tree-ring growth is limited by temperature and spring precipitation (February-April) (see Lhamcoka E site description in Bräuning (2006)). Therefore the early wood formation is negatively affected by the spring conditions, leading to growth reduction of the annual growth rings. Due to the steep slope angle of more than 30° and well drained substrate properties at the study site, ground water influence can be excluded. Therefore we assume the trees δ^{18}O source water properties are mainly controlled by the oxygen isotope configuration of summer precipitation, although it is known that snow derived melt water input affects the source water properties of trees (Treydte et al., 2006). According to dry and cold winter monsoon conditions, a well developed snow cover at our study site is not likely. Hence, 13% of potential solid precipitation during October and April might not affect the source water properties at our study site remarkable.

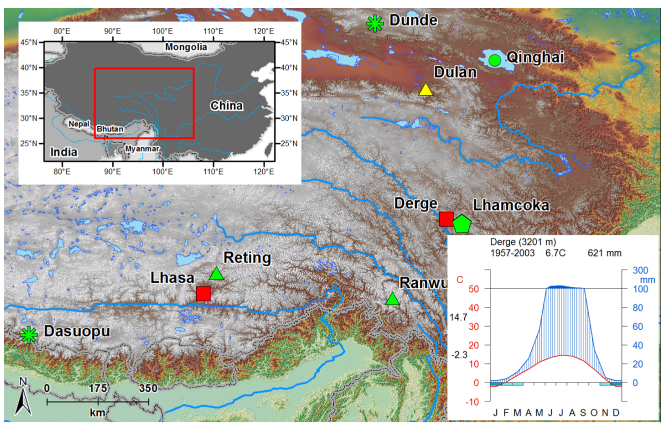

Fig. 1. Location of the study site Lhamcoka (green pentagon) and other proxy archives mentioned in the text. Green triangles: tree-ring δ^{18}O chronologies; Yellow triangle: tree-ring width chronology; Green flake: ice cores; Green circle: Lake sediments. Red rectangles indicate climate stations.

Lhamcoka is influenced by the Indian Summer Monsoon system with typical maxima of temperature and precipitation during the summer months (see climate diagram in Figure

1). The nearby climate station Derge (3201m absl, 50km distance to sampling site) records 78% (541mm) of its annual precipitation between June and September which is in accordance to common monsoonal climate properties (Böhner, 2006). The Derge climate record (data provided by China Meteorological Administration) revealed increasing temperatures of about 0.6°C during the period 1956-1996, whereas the amount and interannual variability of precipitation remains constant within these 41 years.

Five trees were chosen for isotope analysis, to adequately capture inter-tree variability of $\delta^{18}O$ (Leavitt, 2010). The trees were selected according to (i) old age of the cores to maximize the length of the derived reconstruction, (ii) avoidance of growth asymmetries due to slope processes, (iii) sufficient amounts of material (samples with wider rings were favoured), and (iv) a high inter-correlation among the tree-ring width series of the respective cores.

2.2 Sample preparation

We used the tree-ring width master chronology of Bräuning (2006) in order to date each annual ring precisely. The dated tree-rings were cut with a razor blade under a microscope. $\delta^{18}O$ values were measured from each tree individually in annual resolution. During periods of the chronology with extremely narrow rings, we used shifted block pooling to obtain sufficient material (Böttger and Friedrich, 2009). Pooling was applied between the years 1864-1707 (see chronology parts with missing EPS in Figure 2). To obtain pure α-cellulose, we followed the chemical treatment presented in Wieloch et al. (2011). The α-cellulose was homogenised with an ultrasonic unit and the freeze dried material was loaded into silver capsules (Laumer et al., 2009). The ratio of $^{18}O/^{16}O$ was determined in a continuous flow mass spectrometer (Delta V Advantage; Thermo Fisher Scientific Inc.). The standard deviation for the repeated measurement of an internal standard was better than 0.25‰.

2.3 Statistical analyses

We used standard dendrochronology techniques of chronology building, model building and verification for the purpose of a reliable climate reconstruction (Cook and Kairiukstis, 1990). All analysis were conducted with the open source statistical software R (http://cran.r-project.org/). The stable isotope chronology was calculated within the "dplR" package developed by Bunn (2008) and the dendroclimatological correlation and response analyses were conducted by the "bootRes" package (Zang and Biondi, 2012). The pooling method we executed required a running mean calculation. Thus, the presented chronology has a quasi annual resolution, smoothed with a five years running mean filter. To evaluate the isotope chronology reliability the Expressed Population Signal (EPS, introduced by Wigley et al. (1984)) and the Gleichläufigkeit (GLK) were computed. The EPS expresses the variance fraction of a chronology in comparison with a theoretically infinite tree population, whereas the GLK specifies the proportion of agreements/disagreements of interannual growth tendencies among the trees of the study site. The EPS is interrupted within our $\delta^{18}O$ chronology at parts were we applied shifted block pooling.

3 Results

3.1 Chronology characteristics

The Lhamcoka $\delta^{18}O$ chronology is defined by a mean of 21.27‰ and global minima/maxima of 18.24‰/ 24.83‰, respectively. The values are similar to results from nearby studies (An et al. (2014); Liu et al. (2012); Liu et al. (2013)). Moreover, the trees within the chronology are characterized by a common signal that is expressed in an EPS of 0.88 and a highly significant GLK of 0.57 ($p < 0.01$). Thus, we consider a common forcing among all trees and therefore a reliable mean $\delta^{18}O$ chronology. The chronology can be sub-divided into two parts (see Figure 2). The younger section (1868-1996) shows a pronounced trend of about 2‰ towards heavy isotope ratios. Within this segment the year with the most heavy ratio was detected in 1943 (24.8‰). Before the late 1870s the isotope $\delta^{18}O$ values oscillate around the chronology mean. A phase of considerable low $\delta^{18}O$ values is obvious from 1200 to 1300. Within this section the lightest isotope ratio was detected in 1272 (18.2‰). The signal strength (EPS) occasionally drops below the commonly accepted threshold of 0.85 during several periods. One reason might be the imprecise cutting of very narrow rings (ring width <0.2 mm). A mix of several rings produces a signal that cannot be related with certainty to a specific year, a problem well known when using very old trees (Berkelhammer and Stott (2012); Xu et al. (2013)). Nevertheless we have confidence in the Lhamcoka chronology due to an EPS above the threshold during the period 1300-1700 AD.

3.2 Climatic response of tree-ring stable oxygen isotopes

We conducted linear correlation analyses between the $\delta^{18}O$ values and monthly climate data as well as calculated seasonal means of climate elements. The available climate record of station Derge covers 41 years (1956-1996 AD) and correlations were calculated for temperature (mean), precipitation, relative humidity, sunshine hours (duration of global radiation >120W/m²), and vapour pressure (see Figure 3).

Summer moisture conditions explain most of the variance of the $\delta^{18}O$ chronology during the calibration period (1956-1996 AD). The stable oxygen isotopes are highly significantly ($p<0.01$) correlated with precipitation, relative humidity, sunshine hours and vapour pressure during July and

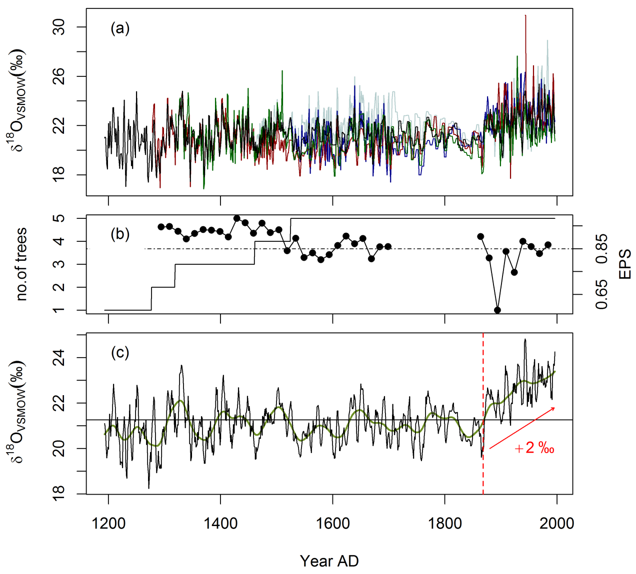

Fig. 2. Lhamcoka tree-ring δ^{18}O isotope chronology. (a) Individual δ^{18}O time series of five individuals. The coarse resolution between 1867 and 1707 results from shifted block pooling. (b) Running EPS (calculated for 25 year intervals, lagged by 10 years) and number of trees used for the reconstruction (solid line). Dashed line represents the theoretical EPS threshold of 0.85. (c) Tree-ring δ^{18}O chronology spanning the period 1193-1996 (AD). Green solid line represents a 50-year smoothing spline. Red dashed line marks the turning point towards heavier isotope ratios after ~1870.

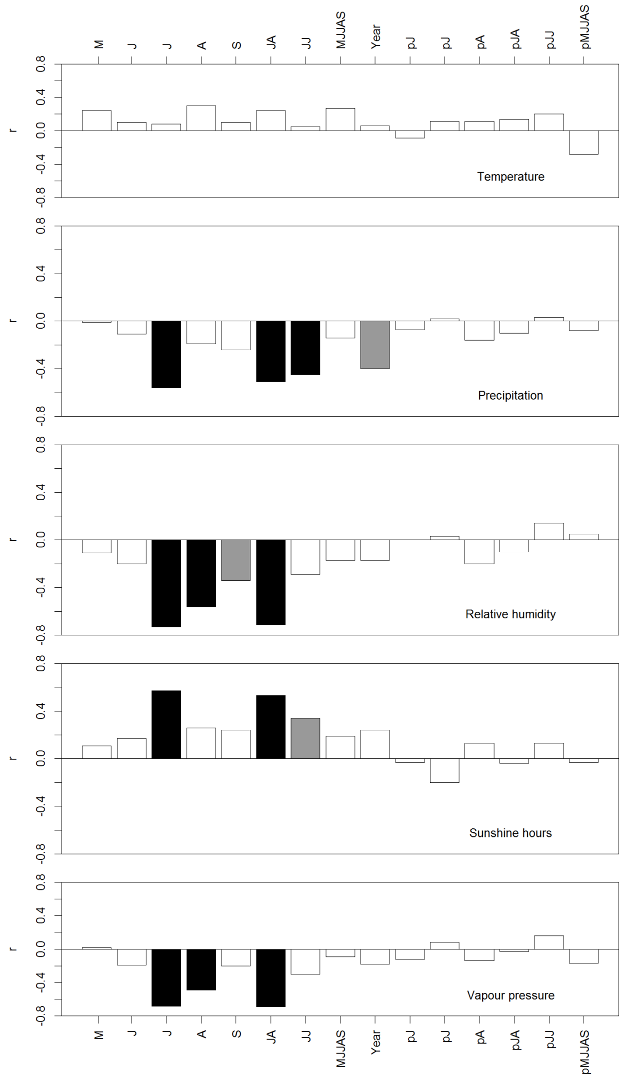

Fig. 3. Response of tree-ring δ^{18}O to monthly/seasonal temperature, precipitation, relative humidity, sunshine hours and vapour pressure over the period 1956-1996 AD. Gray and black bars indicate correlations significant at p<0.05 and p<0.01, respectively; p indicates months/seasons of the previous year.

August. Highest (negative) correlations were obtained with relative humidity during July (r= -0.73) and July/August (r= -0.71). Thus, if relative humidity is high, transpiration is lowered and the depletion of light δ^{16}O due to leaf water fractionation is reduced. Additionally, weak and non-significant relationships were found with the mean temperature in all months/seasons. Thus, concepts of integrated temperature-moisture indexes, e.g. the vapour pressure difference (VPD: Kahmen et al. (2011)), are unlikely to explain more of the variance in our data. However, we calculated the VPD as the difference between water vapour saturation pressure (E) and vapour pressure (e) and correlated the VPD time series against the δ^{18}O during the calibration period. Therewith we obtained significant but slightly weaker relationships with VPD (r = 0.68, p <0.01), since relative humidity and VPD are both influenced by temperature. Moreover, sunshine hours are positively related to the δ^{18}O variation. This association of high sunshine hours, less cloudiness, decreased relative humidity and thus increased δ^{18}O values was corroborated by findings for southeast Tibet (Shi et al., 2012). Very weak correlations were found with climate conditions during the previous year. Therefore, plant physiological carry over effects as well as stagnating soil water can be regarded as inferior factors for tree-ring δ^{18}O variations. The explained variance of linear regressions between stable oxygen isotopes and relative humidity accounts for 53%. Hence, the δ^{18}O value mainly depends on relative humidity, which is in accordance to findings of Roden and Ehleringer (2000). Although highest correlations were obtained with single months (July: r = -0.73 (p<0.01)), the reconstruction was established for the summer season (mean relative humidity of July and August). In terms of using wood cellulose of a single year, the humidity reconstruction of the major growing season is more robust than for single months.

3.3 Reconstruction of relative humidity

We employed a linear model for the reconstruction of relative humidity over the past 800 years. The linear relationship was achieved for the δ^{18}O values and instrumental records of relative humidity at climate station Derge between 1956-1996 AD. The model was validated according to standard methods presented in Cook and Kairiukstis (1990) and Cook et al. (1994). We applied the leave-one-out validation procedure due to the short time period of available climate data. The model statistics are summarized in Table 1.

Table 1. Verification statistics according to the linear transfer model of δ^{18}O and relative humidity within the calibration period 1956-1996 AD.

Sign-test (ST)	0.73 ($p<0.1$)
Product-moment correlation (PMC)	0.67 ($p<0.01$)
Product means test (PMT)	3.3 ($p<0.01$)
Reduction of Error (RE)	0.45
Coefficient of efficiency (CE)	0.45

The validation tests indicated that (1) the number of agreements between the reconstructed climate series and the meteorological record is according to the sign orientation significantly different from a pure chance driven binomial test (ST); (2) the cross-correlation between the reconstruction and the measurement is highly significant (PMC, PMT) and (3) the reconstruction is reliable due to a positive RE and CE, indicating the reconstruction is better than the calibration period mean (Cook et al., 1994). Thus, our linear model is suitable for climate reconstruction purposes. The model related to the reconstruction of summer relative humidity is described as: $rh_{JA} = -2.3 * \delta^{18}O + 125.3$ (rh_{JA}, expressed in %). A negative relationship between tree-ring stable oxygen isotopes and relative humidity was documented properly in several studies around the globe and among different species (Anderson et al. (1998); Burk and Stuiver (1981); Ramesh et al. (1986); Tsuji et al. (2006)). However, due to varying environmental settings (e.g. climate, soil) and different biological leaf properties (Kahmen et al., 2009), the slopes of the regression function differ significantly among study sites and species. Hence, δ^{18}O inferred model parameters from a neighboring summer relative humidity reconstruction (June-August) using Abies trees differ from our regression model (An et al., 2014). Our reconstruction reveals several phases of high and low summer humidity (see Figure 4). Negative deviations from the mean value (72.4%; sd = 4.9%) occurred during 1300-1345, 1475-1525, 1630-1670 and 1866-1996 (periods are emphasized with dashed vertical lines in Figure 4). The most pronounced relative humidity depression started in the late 1870s (dashed red line in Figure 4) and lasts until the ~1950s. The period is characterized by the driest summer in 1943 (rh = 68.4%). The remarkable moisture reduction since the end of the LIA has been validated for the southern and south-eastern part of the TP (Liu et al. (2014); Xu et al. (2012); Zhao and Moore (2006)). After the ~1950s a clear trend towards even drier conditions is attenuated (trend slope = 0.01, p = 0.63). This finding is in accordance with results from the central and southeastern TP (Grießinger et al. (2011); Liu et al. (2013); Shi et al. (2012)) and might be caused by uneven warming trends of the northern and equatorial Indian Ocean sea surface temperatures (Chung and Ramanathan, 2006). More humid periods were detected during 1193-1300, 1345-1390, 1455-1475 and 1740-1750, with the highest relative humidity in 1272 (rh = 83.5%), respectively. Thus, the MWP is characterized by the highest humidity values within the past 800 years. Similar conditions were observed for Inner Asia and the northern TP (Pederson et al. (2014); Yang et al. (2013)) but were not corroborated for the central TP (Grießinger et al., 2011). The moderate oscillation of our humidity reconstruction during the LIA contrasts results of increasing and decreasing moisture trends at different parts of the TP (Grießinger et al. (2011); Shao et al. (2005); Yao et al. (2008)). We identified extreme inter-annual humidity variations by calculating the third standard deviation of the first differences. Years with humidity variations above 10% were detected in 1960/1961, 1946/1947, 1941/1942, 1706/1707, 1253/1254, 1238/1239, 1233/1234, 1230/1231 and 1225/1226.

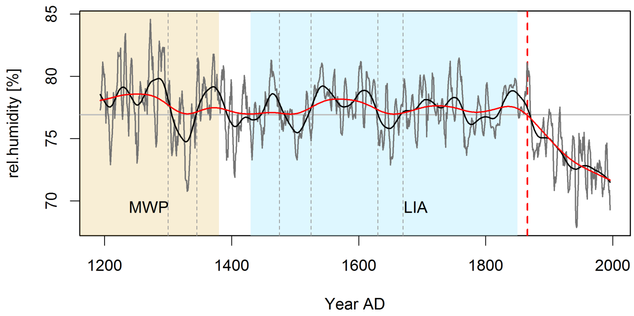

Fig. 4. Summer (July+August) relative humidity reconstruction 1193-1996 AD for the eastern TP. Solid black and red lines represent 50-year and 150-year smoothing splines, respectively. Red dashed line emphasises the turning point towards drier conditions (~1870s). The horizontal gray line illustrates mean relative summer humidity (rh = 72.4%). Vertical dashed lines are marking relatively dry periods. The Medieval Warm Period (MWP) and Little Ice Age (LIA) are emphasized in yellow and blue.

4 Discussion

Lhamcoka is located at the assumed boundary zone of air masses from the Indian Ocean, South, the North Pacific and Central Asia (Araguás-Araguás et al., 1998). Thus, our study site is likely influenced by the monsoon circulation (Indian and Southeast Asian monsoon) as well as by the westerlies (Morrill et al., 2003). Especially the long term spatio-temporal modulation of the monsoon circulation systems has been intensively studied (e.g. Kumar et al. (1999); Wang et al. (2012); Webster et al. (1998)) and may significantly control the moisture availability at our study site. The pre-condition for the formation of the monsoon is the land-sea surface temperature gradient between the Asian land mass and the surrounding oceans (Kumar et al., 1999). However, the monsoon circulation system shows variations at interannual and intraseasonal timescales (Webster et al., 1998). In particular, the ENSO impact on the monsoon circulation has been studied extensively (e.g. Cherchi and Navarra (2013); Kumar et al. (2006); Park and Chiang (2010)). We tested the influence of ENSO on our humidity reconstruction and achieved no significant relationships, implying an ENSO decoupled climate variability at our proxy site (see interactive discussion of this paper Wernicke et al. (2014)). On an intraseasonal timescale the Madden-Julian-Oscillation (MJO) modulates the monsoonal precipitation (Madden and Julian, 1994), where the 30-90 days zonal propagation of cloud clusters causes breaks and strengthening of the monsoonal precipitation (Zhang, 2005). More recently, the monsoon circulation system has been affected by greenhouse gas and aerosol emissions (Hu et al. (2000); Lau et al. (2006)). Both induce a positive anomaly of monsoonal precipitation due to the strengthening of the thermal gradient in the upper troposphere.

However, in this study we primarily focus on the controls of relative humidity at our study site, rather than targeting large-scale atmospheric circulation influences immediately. Therefore we conducted correlation analysis of the July-August relative humidity at the grid cell of our study site with the July-August relative humidity in the area of 0°-45°N/40°-120°E (ERA Interim data: http://apps.ecmwf.int/datasets/data). Beforehand, we examined the accordance of our summer relative reconstruction and the ERA interim data (mean relative humidity July-August). The significant relationship ($r = 0.77$, $p < 0.01$) suggests that the ERA interim data are likely to represent our relative humidity reconstruction. As shown in figure 5 (A), significant correlations at the 500hPa pressure level are found with almost the entire TP. This suggests a regional signal, reflecting the strong connection of moisture variability at our study site with moisture variability over the whole TP. However, significant negative relationships were found with the southwest and southeast Asian regions. These correlations are even more evident on the 300hPa level (Figure 5 (B)) and show a remarkable spatial pattern. Interestingly, the negative correlation in southwest Asia contains the region where Ding and Wang (2005) defined an index for the westerly wave activity (west central Asia: 60°-70°E /35°-40°N). The significance of this finding is corroborated by strong correlations of the mean summer relative humidity in 200hPa of the west central Asian region and our proxy record ($r = -0.58$, $p < 0.05$). Several studies highlight the general influence of the ASM as the major driver for Tibetan moisture variability (Araguás-Araguás et al. (1998); Hren et al. (2009); Tian et al. (2007)). However, the results of Ding and Wang (2005), Saeed et al. (2011) or Mölg et al. (2014) and our findings indicate that the mid-latitude westerlies influence should be be taken into consideration in future studies.

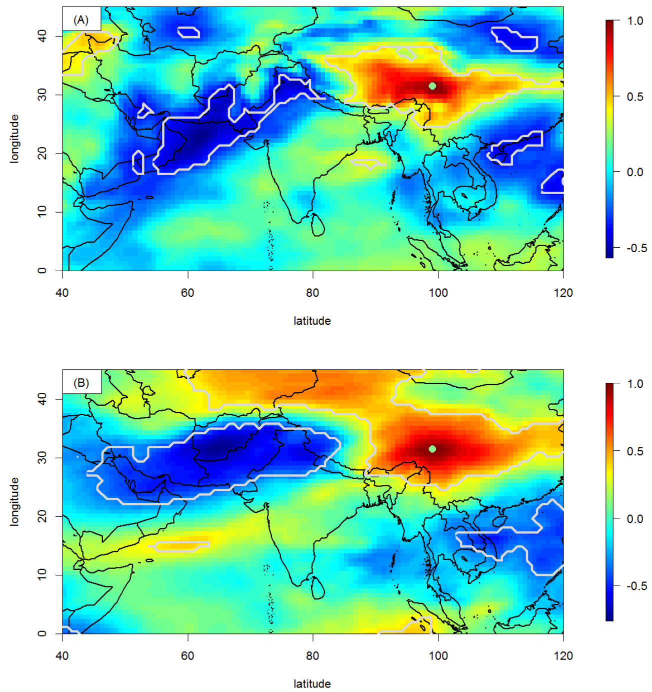

Fig. 5. Spatial correlation of July-August relative humidity (ERA interim data, 1979-2013) at the (A) 500hPa and (B) 300 hPa pressure level. Color code represents the Pearson correlation coefficient. White lines delineate the 95% significance level. Proxy location is shown by the light green dot.

For an analysis of the regional representativeness of our data set, we compared the Lhamcoka $\delta^{18}O$ chronology with six moisture sensitive proxies from the TP (see Figure 7 and locations in Figure 1), including normalized tree-ring (TR) $\delta^{18}O$ records (Ranwu TR: Liu et al. (2013); Reting TR: Grießinger et al. (2011)), tree-ring width data (Dulan TR: Sheppard et al. (2004)), accumulation records (Dasuopu and Dunde ice cores: Thompson et al. (2000) and lake sediments (Qinghai Sediment: Xu et al. (2006a)). We found significant positive correlations between our time series and the Ranwu ($r = 0.55$, $p < 0.01$), Reting ($r = 0.23$, $p < 0.01$), Dunde ($r = 0.16$, $p < 0.01$) and Qinghai ($r = 0.22$, $p < 0.1$) data sets. Only the tree-ring width series of Dulan is negatively correlated to the $\delta^{18}O$ values of Lhamcoka ($r = -0.16$, $p < 0.01$). The snow accumulation rate of Dasuopu ice core has no relationship to our $\delta^{18}O$ chronology ($r = -0.04$, $p = 0.3$). In case of weak correlations ($|r| < 0.2$) and due to the degrees of freedom (DF >100), significance levels alone might be misleading and indicate only a statistical and not a causal relationship. However, strong relationships between the tree-ring δ^{18}O chronologies of Lhamcoka and Ranwu, and partly Reting, are reasonable, since moisture reconstructions from these sites rely on the same proxy (δ^{18}O of tree-ring cellulose) and the trees grew under similar climate conditions. Relationships to the more northern located sites (Dunde, Dulan, Qinghai) are difficult to verify, according to a clearly detectable westerly influence at these sites. We adapted the color scheme of figure 4 and highlighted the MWP (yellow polygon), LIA (blue polygon), and the remarkable humidity decline since the late 1870s (dashed red line) in figure 7. The MWP is characterized by more humid conditions on the eastern TP (Lhamcoka), a drier phase on the central plateau (Reting) and moderate humidity conditions on the northern plateau (Dulan). During the LIA a remarkable moisture increase occurred at the central and southern plateau (Reting, Dasuopu). Although humidity was high according to these archives, the ASM was weak during that time (Anderson et al. (2002); Gupta et al. (2003)).

Thus, the findings for Reting and Dasuopu revealed moisture conditions during cold phases and even drier circumstances during warm periods which might be contrary to findings of Meehl (1994) and Zhang and Qiu (2007)). The sudden moisture decrease since the late 1870s affects the eastern (Lhamcoka), southern (Dasuopu), and central (Reting) parts of the TP. Reasons for the sudden moisture decline were discussed in detail by Xu et al. (2012). They address the moisture decrease to the reduction in the thermal gradient induced by uneven land-ocean temperature rise, caused by aerosol and greenhouse gas loads. In fact, under rising north hemispheric air temperatures (Shi et al., 2013) the air moisture load over sea is increased but due to solar dimming effects of black aerosols, the northeastward moisture transport is hampered (Sun et al., 2010). In addition, Zhao and Moore (2006) attributed the moisture decline to the "weakening of the easterly trade wind system along the equatorial Pacific since the middle of 19th century". Moreover, decreasing varve thicknesses imply a weakening Asian summer monsoon in the past 160 years (Chu et al., 2011). The latter analysis revealed a link to warm phases of ENSO and an anomalous regional Hadley circulation. However, their explanation approach remains incomplete due to dynamic issues associated with rising temperatures and a weakening South Asian summer monsoon. Therewith a terminal explanation is not given yet and should be discussed in future studies.

In comparison to tree-ring sites located further south (e.g. Liu et al. (2013); Sano et al. (2013); Shi et al. (2012)), the distinct humidity decline is more pronounced on the central and eastern TP. Sano et al. (2013) concluded from that observation a weakening of the monsoon since the last 100-200 years due to uneven SST variation (equatorial vs. northern Indian Ocean regions). To test this hypothesis, we calculated the averaged SST anomalies of the equatorial and northern Indian

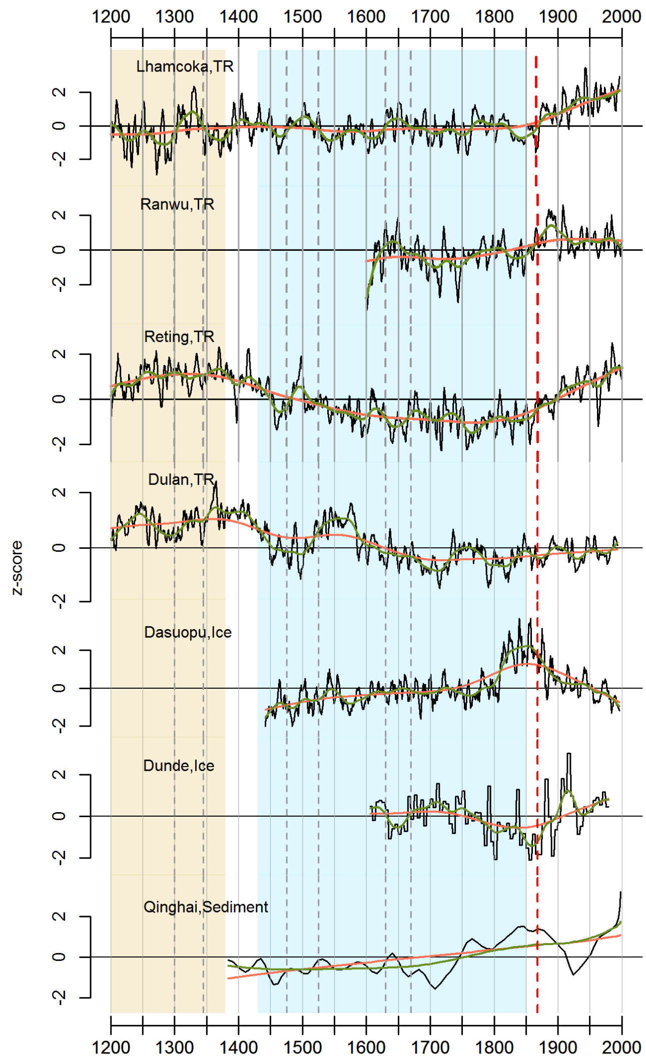

Fig. 6. Multiproxy comparison of tree-ring data (TR), ice core and lake sediment data. TR: Lhamcoka: this study; Ranwu: Liu et al. (2013) ; Reting: Grießinger et al. (2011) ; Dulan: Sheppard et al. (2004). Ice: Dasuopu and Dunde: Thompson et al. (2000). Sediment: Qinghai: Xu et al. (2006a). Locations of the several proxies are shown in Fig. 1. Z-scores were derived from raw proxy data and not from reconstructions. High positive z-scores indicating dry conditions for TR and sediment records, whereas high z-scores of ice accumulations represent humid conditions, respectively.

Ocean (52.5°-112.5°E /2.5°N-2.5°S; 52.5°-112.5°E /22.5°-27.5°N). As shown in figure 7, a slight SST increase in both regions since ~1950s is obvious. Besides, the gradient constantly decreases, but restrengthens since ~1970s. This finding contrasts with a generally weakening monsoon circulation since the past 100-200 years deduced from a thermal gradient reduction. Therefore, the various moisture variations of the southern and central/eastern TP during the last 100-200 years might be evoked by varying local air mass characteristics.

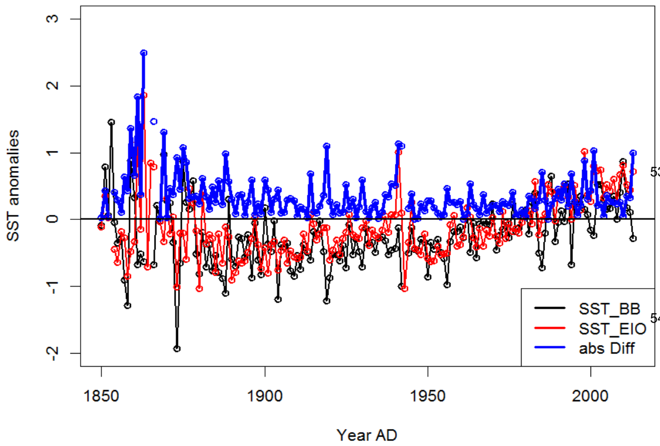

Fig. 7. Sea surface temperature anomalies in different regions of the Indian Ocean: Bay of Bengal-North Indian ocean (SST BB: 52.5°-112.5°E/22.5°-27.5°N) and equatorial Indian Ocean (SST EIO: 52.5°-112.5°E/2.5°N-2.5°S) (Rayner et al., 2006). Difference between the two time series is marked with a blue line.

5 Conclusions

We demonstrated that our 800 years long δ^{18}O chronology is suitable for a reliable reconstruction of summer relative humidity. Long-term air humidity variations revealed more humid conditions during the termination of the MWP, relatively stable humidity during the LIA and a sudden decrease in summer humidity since the 1870s. After the ~1950s the trend towards more heavy oxygen isotope ratios is mitigated due to the restrengthening of the ISM. These findings are in accordance with other reconstructions of moisture conditions for the central and eastern TP. Spatial correlations indicate a significant relationship of summer relative humidity at our study site and major parts of the TP. Additionally, a negative correlation within the higher atmosphere over the west central Asia region imply a westerly influence. Furthermore, the thermal contrast between the equatorial and northern Indian Ocean, which is assumed to control moisture supply during the ISM, is slightly stable over time. Thus, to comprehensively indicate reasons for the distinct ~1870s moisture decline more detailed climate dynamic studies and highly-resolved spatio-temporal hydroclimate reconstructions are needed.

Acknowledgements. The authors thank the German Federal Ministry of Education and Research (BMBF) for the financial support. We also thank Roswitha Höfner-Stich for her efficient and precise work at the mass spectrometer. We additionally like to thank Prof. Dr. Thomas Mölg for his inspiring and helpful suggestions.

References

An, W., Liu, X., Leavitt, S., Xu, G., Zeng, X., Wang, W., Qin, D., and Ren, J.: Relative humidity history on the Batang–Litang Plateau of western China since 1755 reconstructed from tree-ring δ^{18}O and δD, Climate Dynamics, 42, 2639–2654, doi:10.1007/s00382-013-1937-z, 2014.

Anderson, D., Overpeck, J., and Gupta, A.: Increase in the Asian Southwest Monsoon During the Past Four Centuries, Science, 297, 596–599, doi:10.1126/science.1072881, 2002.

Anderson, W., Bernasconi, S., and McKenzie, J.: Oxygen and carbon isotopic record of climatic variability in tree ring cellulose (Picea abies)' An example from central Switzerland (1913-1995), Journal of Geophysical Research, 103, 31 625–31 636, 1998.

Araguás-Araguás, L., Fröhlich, K., and Rozanski, K.: Stable isotope composition of precipitation over southeast Asia, Journal of Geophysical Research Letters, 103, 721–728, 1998.

Berkelhammer, M. and Stott, L.: Secular temperature trends for the southern Rocky Mountains over the last five centuries, Geophysical Research Letters, 39, 1–6, doi:10.1029/2012GL052447,, 2012.

Böhner, J.: General climatic controls and topoclimatic variations in Central and High Asia, Boreas, 35, 279–295, 2006.

Bollasina, M., Ming, Y., and Ramaswamy, V.: Anthropogenic aerosols and the weakening of the South Asian Summer Monsoon, Science, 334, 502–505, doi:10.1126/science.1204994, 2011.

Bräuning, A.: Climate history of the Tibetan Plateau during the last 1000 years derived from a network of Juniper chronologies, Dendrochronologia, 19, 127–137, 2001.

Bräuning, A.: Tree-ring evidence of "Little Ice Age" glacier advances in southern Tibet, The Holocene, 16, 369–380, 2006.

Böttger, T. and Friedrich, M.: A new serial pooling method of shifted tree ring blocks to construct millennia long tree ring isotope chronologies with annual resolution, Isotopes in Environmental and Health Studies, 45, 68–80, 2009.

Bunn, A.: A dendrochronology program library in R (dplR), Dendrochronologia, 26, 115–124, doi:10.1016/j.dendro.2008.01.002, 2008.

Burk, R. and Stuiver, M.: Oxygen isotope ratios in trees reflect mean annual temperature and humidity, Science, 27, 1417–1419, 1981.

Cherchi, A. and Navarra, A.: Influence of ENSO and of the Indian Ocean Dipole on the Indian summer monsoon variability, Climate Dynamics, 41, 81–103, doi:0.1007/s00382-012-1602-y, 2013.

Chu, G., Sun, Q., Yang, K., Li, A., Yu, X., Xu, T., Yan, F., Qang, X., Xie, M., Lin, Y., and Liu, Q.: Evidence for decreasing South Asian summer monsoon in the past 160 years from varved sediment in Lake Xinluhai, Tibetan Plateau, Journal of Geophysical Research, 116, doi:10.1029/2010JD014454, 2011.

Chung, C. and Ramanathan, V.: Weakening of north Indian SST gradients and the Monsoon rainfall in India and the Sahel, Journal of Climate, 19, 2036–2045, 2006.

Cook, E. and Kairiukstis, L.: Methods of dendrochronology, Kluwer Academic Publishers, Dordrecht, Boston, London, 1990.

Cook, E., Briffa, K., and Jones, P.: Spatial regression methods in dendroclimatology: A review and comparison of two techniques, International Journal of Climatology, 14, 379–402, 1994.

Cook, E., Anchukaitis, K., Buckley, B., D'Arrigo, R., Jacoby, G., and Wright, W.: Asian Monsoon Failure and Megadrought During the Last Millennium, Science, 328, 486–489, doi:10.1126/science.1185188, 2010.

Ding, Q. and Wang, B.: Circumglobal teleconnection in the northern hemisphere summer, Journal of climate, 18, 3483–3505, 2005.

Esper, J., Frank, D., Battipaglia, G., Büntgen, U., Holert, C., Treydte, K., Siegwolf, R., and Saurer, M.: Low-frequency noise in δ^{13}C and δ^{18}O tree ring data: A case study of Pinus uncinata in the Spanish Pyrenees, Global Biogeochemical Cycles, 24, 1–11, doi:10.1029/2010GB003772, 2010.

Grießinger, J., Bräuning, A., Helle, G., Thomas, A., and Schleser, G.: Late Holocene Asian summer monsoon variability reflected by δ^{18}O in tree-rings from Tibetan junipers, Geophysical Research Letters, 38, 1–5, doi:10.1029/2010GL045988, 2011.

Gupta, A., Anderson, D., and Overpeck, J.: Abrupt changes in the Asian southwest monsoon during the Holocene and their links to the North Atlantic Ocean, Nature, 421, 354–357, 2003.

Hren, M., Bookhagen, B., Blisniuk, P., Booth, A., and Chamberlain, C.: δ^{18}O and δD of streamwaters across the Himalaya and Tibetan Plateau: Implications for moisture sources and paleoelevation reconstructions, Earth and Planetary Science Letters, 288, 20–32, doi:10.1016/j.epsl.2009.08.041, 2009.

Hu, Z.-Z., Latif, M., Roeckner, E., and Bengtsson, L.: Intensified Asian summer monsoon and its variability in a coupled model forced by increasing greenhouse gas concentrations, Geophysical Research Letters, 27, 2681–2684, 2000.

Immerzeel, W., van Beek, L., and Bierkens, M.: Climate Change will affect the Asia Water Towers, Science, 328, 1382–1385, doi:10.1126/science.1183188, 2010.

Kahmen, A., Simonin, K., Tu, K., Goldsmith, G., and Dawson, T.: The influence of species and growing conditions on the 18-O enrichment of leaf water and its impact on 'effective path length', New Phytologist, 184, 619–630, doi:10.1111/j.1469-8137.2009.03008.x, 2009.

Kahmen, A., Sachse, D., Arndt, S., Tu, K., Farrington, H., Vitousek, P., and Dawson, T.: Cellulose δ^{18}O is an index of leaf-to-air vapor pressure difference (VPD) in tropical plants, Proceedings of the National Academy of Sciences, 108, 1981–1986, www.pnas.org/cgi/doi/10.1073/pnas.1018906108, 2011.

Kumar, K., Rajagopalan, B., and Cane, M.: On the weakening relationship Between the Indian Monsoon and ENSO, Science, 284, 2156–2159, doi:10.1126/science.284.5423.2156, 1999.

Kumar, K., Rajagopalan, B., Hoerling, M., Bates, G., and Cane, M.: Unraveling the mystery of Indian Monsoon failure during El Nino, Science, 314, 115–119, doi:10.1126/science.1131152, 2006.

Lau, K., Kim, M., and Kim, K.: Asian summer monsoon anomalies induced by aerosol direct forcing: the role of the Tibetan Plateau, Climate Dynamics, 26, 855–864, doi:10.1007/s00382-006-0114-z, 2006.

Laumer, W., Andreau, L., Helle, G., Schleser, G., Wieloch, T., and Wissel, H.: A novel approach for the homogenization of cellulose to use micro-amounts for stable isotope analyses, Rapid Communications in Mass Spectrometry, 23, 1934–1940, doi:10.1002/rcm.4105, 2009.

Leavitt, S.: Tree-ring C-H-O isotope variability and sampling, Science of the Total Environment, 408, 5244–5253, 2010.

Liu, X., An, W., Treydte, K., Shao, X., Leavitt, S., Hou, S., Chen, T., Sun, W., and Qin, D.: Tree-ring δ^{18}O in southwestern China linked to variations in regional cloud cover and tropical sea surface temperature, Chemical Geology, 291, 104–115, doi:10.1016/j.chemgeo.2011.10.001, 2012.

Liu, X., Zeng, X., Leavitt, S., Wang, W., An, W., Xu, G., Sun, W., Wang, Y., Qin, D., and Ren, J.: A 400-year tree-ring δ^{18}O chronology for the southeastern Tibetan Plateau: Implications for inferring variations of the regional hydroclimate, Global and Planetary Change, 104, 23–33, doi:10.1016/j.gloplacha.2013.02.005, 2013.

Liu, X., Xu, G., Grießinger, J., An, W., Wang, W., Zeng, X., Wu, G., and Qin, D.: A shift in cloud cover over the southeastern Tibetan Plateau since 1600: Evidence from regional tree-ring δ^{18}O and its linkages to tropical oceans, Quaternary Science Reviews, 88, 55–68, doi:10.1016/j.quascirev.2014.01.009, 2014.

Liu, Y., Cai, Q., Liu, W., Yang, Y., Sun, J., Song, H., and Li, X.: Monsoon precipitation variation recorded by tree-ring δ^{18}O in arid Northwest China since AD 1878, Chemical Geology, 252, 56–61, doi:10.1016/j.chemgeo.2008.01.024, 2008.

Madden, R. and Julian, P.: Observations of the 40-50 day Tropical Oscillation- A review, Monthly weather review, 122, 814–837, 1994.

Maussion, F., Scherer, D., Mölg, T., Collier, E., Curio, J., and Finkelnburg, R.: Precipitation seasonality and variability over the Tibetan Plateau as resolved by the High Asia Reanalysis, Journal of Climate, 27, 1910–1927, doi:10.1175/JCLI-D-13-00282.1, 2014.

McCarroll, D. and Loader, N.: Stable isotopes in tree rings, Quaternary Science Review, 23, 771–801, 2004.

Meehl, G.: Influence of the land surface in the Asian Summer Monsoon: External conditions versus internal feedbacks, Journal of Climate, 7, 1033–1049, 1994.

Mölg, T., Maussion, F., and Scherer, D.: Mid-latitude westerlies as a driver of glacier variability in monsoonal High Asia, Nature climate change, 4, 68–73, doi:10.1038/NCLIMATE2055, 2014.

Morrill, C., Overpeck, J., and Cole, J.: A synthesis of abrupt changes in the Asian summer monsoon since the last deglaciation, The Holocene, 13, 465–476, 2003.

Park, H.-S. and Chiang, J.: The delayed effect of major El Nino Events on Indian Monsoon Rainfall, Journal of Climate, 23, 932–946, doi:10.1175/2009JCLI2916.1, 2010.

Pederson, N., Hessl, A., Baatarbileg, N., Anchukaitis, K., and Di Cosmo, N.: Pluvials, droughts, the Mongol Empire, and modern Mongolia, Proceedings of the National Academy of Sciences of the United States of America (PNAS), 111, 4375–4379, doi:10.1073/pnas.1318677111/-/DCSupplemental, 2014.

Ramesh, R., Bhattacharya, S., and Gopalan, K.: Climatic correlations in the stable isotope records of silver fir (Abies pindrow) trees from Kashmir, India, Earth and Planetary Science Letters, 79, 66–74, 1986.

Rayner, N., Brohan, P., Parker, D., Folland, C., Kennedy, J., Vanicek, M., Ansell, T., and Tett, S.: Improved analyses of changes and uncertainties in sea surface temperature measured in situ since the mid-nineteenth century: the HadSST2 data set, Journal of Climate, 19, 446–469, 2006.

Roden, J. and Ehleringer, J.: Hydrogen and oxygen isotope ratios of tree ring cellulose for field-grown riparian trees, Oecologia, 123, 481–489, 2000.

Roden, J., Lin, G., and Ehleringer, J.: A mechanistic model for interpretation of hydrogen and oxygen isotope ratios in tree-ring cellulose, Geochimica et Cosmochimica Acta, 64, 21–35, 2000.

Saeed, S., Müller, W., Hagemann, S., and Jacob, D.: Circumglobal wave train and the summer monsoon over northwestern India and Pakistan: the explicit role of the surface heat low, Climate Dynamics, 37, 1045–1060, doi:10.1007/s00382-010-0888-x, 2011.

Sano, M., Sheshshayee, M., Managave, S., Ramesh, R., Sukumar, R., and Sweda, T.: Climatic potential of δ^{18}O of Abies spectabilis from the Nepal Himalaya, Dendrochronologia, 28, 93–98, doi:10.1016/j.dendro.2009.05.005, 2010.

Sano, M., Ramesh, R., Sheshshayee, M., and Sukumar, R.: Increasing aridity over the past 223 years in the Nepal Himalaya inferred from a tree-ring δ^{18}O chronology, The Holocene, 1, 1–9, doi:10.1177/0959683611430338, 2011.

Sano, M., Tshering, P., Komori, J., Fujita, K., Xu, C., and Nakatsuka, T.: May–September precipitation in the Bhutan Himalaya since 1743 as reconstructed from tree ring cellulose δ^{18}O, Journal of Geophysical Research: Atmosphers, 118, 8399–8410, doi:10.1002/jgrd.50664, 2013.

Saurer, M., Aellen, K., and Siegwolf, R.: Correlating δ^{13}C and δ^{18}O in cellulose of trees, Plant, Cell and Environment, 20, 1543–1550, 1997.

Shao, X., Huang, L., Liu, H., Liang, E., Fang, X., and Wang, L.: Reconstruction of precipitation variation from tree rings in recent 1000 years in Delingha, Qinghai, Science in China Ser. D Earth Sciences, 48, 939–949, doi:10.1360/03yd0146, 2005.

Sheppard, P., Tarasov, P., Graumlich, L., Heussner, K.-U., Wagner, M., Österle, H., and Thompson, L.: Annual precipitation since 515 BC reconstructed from living and fossil juniper growth of northeastern Qinghai Province, China, Climate Dynamics, 23, 869–881, 2004.

Shi, C., Daux, V., Zhang, Q.-B., Risi, C., Hou, S.-G., Stievenard, M., Pierre, M., Li, Z., and Masson-Delmotte, V.: Reconstruction of southeast Tibetan Plateau summer climate using tree ring δ^{18}O: moisture variability over the past two centuries, Climate of the Past, 8, 205–213, doi:10.5194/cp-8-205-2012, 2012.

Shi, F., Yang, B., Mairesse, A., von Gunten, L., Li, J., Bräuning, A., Yang, F., and Xiao, X.: Northern Hemisphere temperature reconstruction during the last millennium using multiple annual proxies, Climate Research, 56, 231–244, doi:10.3354/cr01156, 2013.

Sternberg, L.: Oxygen stable isotope ratios of tree-ring cellulose: the next phase of understanding, New Phytologist, 181, 553–562, 2009.

Sun, Y., Ding, Y., and Dai, A.: Changing links between South Asian summer monsoon circulation and tropospheric land-sea thermal contrasts under a warming scenario, Geophysical Research Letters, 37, 1–5, 2010.

Thomas, A. and Herzfeld, U.: REGEOTOP: New climatic data fields for east asia based on localized relief information and geostatistical methods, International Journal of Climatology, 24, 1283–1306, doi:10.1002/joc.1058, 2004.

Thompson, L., Yao, T., Mosley-Thompson, E., Davis, M., Henderson, K., and Lin, P.-N.: A high- resolution millennial record of the South Asian monsoon from Himalayan ice cores, Science, 289, 1916–1919, doi:10.1126/science.289.5486.1916, 2000.

Tian, L., Yao, T., MacClune, K., White, J., Schilla, A., Vaughn, B., Vachon, R., and Ichiyanagi: Stable isotopic variations in west China: A consideration of moisture sources, Journal of Geophysical Research, 112, 1–12, doi:10.1029/2006JD007718, 2007.

Treydte, K., Schleser, G., Helle, G., Frank, D., Winiger, M. Haug, G., and Esper, J.: The twentieth century was the wettest period in northern Pakistan over the past millennium, Nature, 440, 1179–1182, doi:10.1038/nature04743, 2006.

Tsuji, H., Nakatsuka, T., and Takagi, K.: δ^{18}O of tree-ring cellulose in two species (spruce and oak) as proxies of precipitation amount and relative humidity in northern Japan, Chemical Geology, 231, 67–76, doi:10.1016/j.chemgeo.2005.12.011, 2006.

Wang, W., Liu, X., Xu, G., Shao, X., Qin, D., Sun, W., An, W., and Zeng, X.: Moisture variations over the past millennium characterized by Qaidam Basin tree-ring δ^{18}O, Chinese Science Bulletin, 58, 3956–3961, doi:10.1007/s11434-013-5913-0, 2013.

Wang, Y., Jian, Z., and Zhao, P.: Extratropical modulation on Asian summer monsoon at precessional bands, Geophysical Research Letters, 39, 1–6, doi:10.1029/2012GL052553, 2012.

Webster, P., Magana, V., Palmer, T., Shukla, J., Tomas, R., Yanai, M., and Yasunari, T.: Monsoons: Processesp, redictability, and the prospects for prediction, Journal of Geophysical Research, 103, 14 451–14 510, doi:10.1029/97JC02719, 1998.

Wernicke, J., Grießinger, J., Hochreuther, P., and Bräuning, A.: Variability of summer humidity during the past 800 years on the eastern Tibetan Plateau inferred from δ^{18}O of tree-ring cellulose, Climate of the Past Discussion, 10, 3327–3356, doi:10.5194/cpd-10-3327-2014, 2014.

Wieloch, T., Helle, G., Heinrich, I., Voigt, M., and Schyma, P.: A novel device for batch-wise isolation of α-cellulose from small-amount wholewood samples, Dendrochronologia, 29, 115–117, doi:10.1016/j.dendro.2010.08.008, 2011.

Wigley, T., Briffa, K., and Jones, P.: On the Average Value of Correalted Time Series, with Application in Dendroclimatology and Hydrometeorology, Journal of Climate and Applied Meteorology, 23, 201–213, 1984.

Xu, C., Sano, M., and Nakatsuka, T.: A 400-year record of hydroclimate variability and local ENSO history in northern Southeast Asia inferred from tree-ring δ^{18}O, Palaeogeography, Palaeoclimatology, Palaeoecology, 286, 588–598, doi:http://dx.doi.org/10.1016/j.palaeo.2013.06.025, 2013.

Xu, H., Ai, L., Tan, L., and An, Z.: Stable isotopes in bulk carbonates and organic matter in recent sediments of Lake Qinghai and their climatic implications, Chemical Geology, 235, 262–275, doi:10.1016/j.chemgeo.2006.07.005, 2006a.

Xu, H., Hong, Y., Lin, Q., Zhu, Y., Hong, B., and Jiang, H.: Temperature responses to quasi- 100- yr solar variability during the past 6000 years based on $\delta^{18}O$ of peat cellulose in Hongyuan, eastern Qinghai- Tibet plateau, China, Palaeography, Palaeoclimatology, Palaeoecology, 230, 155–164, doi:10.1016/j.palaeo.2005.07.012, 2006b.

Xu, H., Hong, Y., and Hong, B.: Decreasing Asian summer monsoon intensity after 1860 AD in the global warming epoch, Climate Dynamics, 39, 2079–2088, doi:10.1007/s00382-012-1378-0, 2012.

Yang, B., Bräuning, A., and Yafeng, S.: Late Holocene temperature fluctuations on the Tibetan Plateau, Quaternary Science Reviews, 22, 2335–2344, doi:10.1016/S0277-3791(03)00132-X, 2003.

Yang, B., Qin, C., Wang, J., He, M., Melvin, T., Osborn, T., and Briffa, K.: A 3.500-year tree-ring record of annual precipitation on the northeastern Tibetan Plateau, Proceedings of the National Academy of Sciences, 111, 2903–2908, doi:10.1073/pnas.1319238111/-/DCSupplemental., http://www.pnas.org/content/suppl/2014/02/05/1319238111.DCSupplemental, 2013.

Yao, T., Duan, K., Xu, B., Wang, N., Guo, X., and Yang, X.: Ice core precipitation record in central Tibetan plateau since AD 1600, Climate of the Past Discussions, 4, 233–248, 2008.

Zang, C. and Biondi, F.: Dendroclimatic calibration in R: The bootRes package for response and correlation function analysis, Dendrochronologia, 31, 68–74, doi:http://dx.doi.org/10.1016/j.dendro.2012.08.001, http://www.sciencedirect.com/science/article/pii/S1125786512000586, 2012.

Zhang, C.: Madden-Julian oscillation, Reviews of Geophysics, pp. 1–36, 2005.

Zhang, P., Cheng, H., Edwards, R., Chen, F.and Wang, Y., Yang, X., Liu, J., Tan, M., Wang, X., Liu, J., An, C., Dai, Z., Zhou, J., Zhang, D., Jia, J., Jin, L., and Johnson, K.: A test of climate, sun, and culture relationships from an 1810- year chinese cave record, Science, 322, 940–942, 2008.

Zhang, Q.-B. and Qiu, H.: A millennium-long tree-ring chronology of Sabina przewalskii on northeastern Qinghai-Tibetan Plateau, Dendrochronologia, 24, 91–95, doi:10.1016/j.dendro.2006.10.009, 2007.

Zhao, H. and Moore, G.: Reduction in Himalayan snow accumulation and weakening of the trade winds over the Pacific since the 1840s, Geophysical Research Letters, 33, 1–5, doi:10.1029/2006GL027339, 2006.

Zhou, T., Yu, R., Li, H., and Wang, B.: Ocean forcing to changes in global Monsoon precipitation over the recent half-century, Jorunal of climate, 21, 3833–3852, doi:10.1175/2008JCLI2067.1, 2008a.

Zhou, T., Zhang, L., and Li, H.: Changes in global land monsoon area and total rainfall accumulation over the last half century, Geophysical Research Letters, 35, 1–6, doi:10.1029/2008GL034881, 2008b.